

Michal Szyper. "Inductance Measurement."

Copyright 2000 CRC Press LLC. <<http://www.engnetbase.com>>.

Inductance Measurement

- 50.1 Definitions of Inductance
- 50.2 Equivalent Circuits and Inductive Element Models
- 50.3 Measurement Methods
Current-Voltage Methods • Bridge Methods • Differential Methods • Resonance Methods
- 50.4 Instrumentation

Michał Szyper

University of Mining and Metallurgy

Inductance is an electrical parameter that characterizes electric circuit elements (two- or four-terminal networks) that become magnetic field sources when current flows through them. They are called inductors, although inductance is not a unique property of them. Electric current i (A) and magnetic flux Φ (Wb) are interdependent; that is, they are coupled. Inductance is a measurable parameter; therefore, it has a physical dimension, a measurement unit (the henry), as well as reference standards. Inductance is a property of all electrical conductors. It is found as *self-inductance* L of a single conductor and as *mutual inductance* M in the case of two or more conductors. Inductors can vary in construction, but windings in the form of coils are the most frequent. In this case, they have characteristic geometrical dimensions: surface A , length l , and N number of turns of windings. The path of magnetic flux can be specially shaped by magnetic cores. [Figure 50.1](#) shows examples of different inductive elements of electric circuits.

Figures 50.1*a* and *b* present windings with self-inductance made as a coreless coil (*a*), and wound on a ferromagnetic core that is the concentrator of the magnetic field (*b*). A transformer loaded by impedance Z_L and an electromagnet loaded by impedance of eddy currents in the metal board, shown in Figures 50.1*c* and *d*, will have not only self-inductance of windings, but also mutual inductance between windings (*c*) or between winding and eddy currents (*d*). Self-inductances and mutual inductances can be detected in busbars of electric power stations as shown in Figure 50.1*e*, and also on tracks on printed circuit boards as in Figure 50.1*f*. Couplings between currents and electromagnetic fields can be made deliberately but can also be harmful, e.g., due to energy losses caused by eddy currents, or due to electromagnetic disturbances induced in the tracks of printed circuit boards. Inductors made as windings on ferromagnetic cores have numerous other applications.

The presence of a ferromagnetic core changes the shape of a magnetic field and increases inductance; but in the case of closed cores, it also causes nonlinear relations between inductance and current as well as current frequency. Closed magnetic cores then have a nonlinear and ambiguous magnetization characteristic $\Phi(i)$ because of magnetic saturation and hysteresis. Inductances of open magnetic cores with an air gap are mainly dependent on the length of the magnetic path in the air. Real coils made of metal (e.g., copper) wire also show resistance R . However, if resistance is measured at the coil terminals with ac current, it depends not only on the cross-section, length, and resistivity of the wire, but also on losses

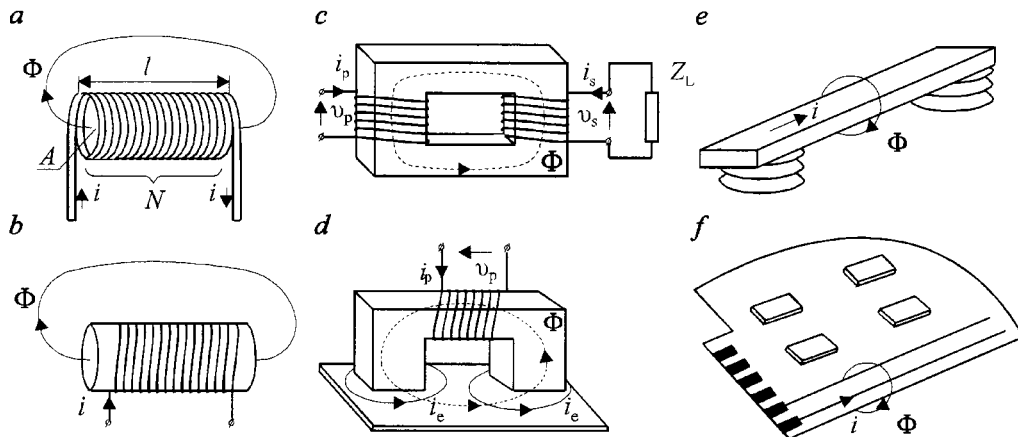


FIGURE 50.1 Examples of different inductive elements: coreless coil (a), coil with ferromagnetic concentrating core (b), transformer (c), electromagnet (d), element of electrical power station bus-bars (e), and printed circuit board with conductive tracks (f).

of active power in the magnetic core. These losses depend on both the current value and frequency. Resistances of inductive elements can also depend on the skin effect. This phenomenon consists of the flow of electric current through a layer of the conductor, near its outer surface, as the result of the effects of the conductor's own magnetic field generated by the current flowing inside the conductor. Notice that the coils have also interturns and stray (to Earth) capacitances C . From its terminals, the inductive elements can then be described by impedances (two-terminal networks) or transmittances (four-terminal networks), values that are experimentally evaluated by current and voltage measurements, or by comparison them with reference impedances. The measured values and the equivalent circuit models of inductive elements are used for evaluation of model parameters: self-inductances, mutual inductances, resistances, and capacitances.

50.1 Definitions of Inductance

Self-inductance is defined as the relation between current i flowing through the coil and voltage v measured at its terminals [1].

$$v = L \frac{di}{dt} \quad (50.1)$$

Using Equation 50.1, the unit of inductance, i.e., the henry, can be defined as follows:

One henry (1 H) is the inductance of a circuit in which an electromotive force of one volt (1 V) is induced, when the current in the circuit changes uniformly by one ampere (1 A) per second (1 s).

The definition of the unit implies the use of uniform-ramp current excitation (the derivative is constant); in practice, however, mainly sinusoidal current excitation is used in inductance measurement.

Mutual inductance M of windings coupled by magnetic flux Φ is a parameter that depends on the coupling coefficient. The coupling coefficient is defined as *perfect coupling* in the case in which the total flux of one winding links the second one; *partial coupling* is the case in which only a fraction of flux links the second one; and *zero coupling* is the case in which no part of the flux of one winding links the second one. Assuming that, as in Figure 50.1c, the second N_s winding is not loaded (i.e., $i_s = 0$) and the flux Φ is a part of the total flux produced by current i_p , then voltage v_s is described by:

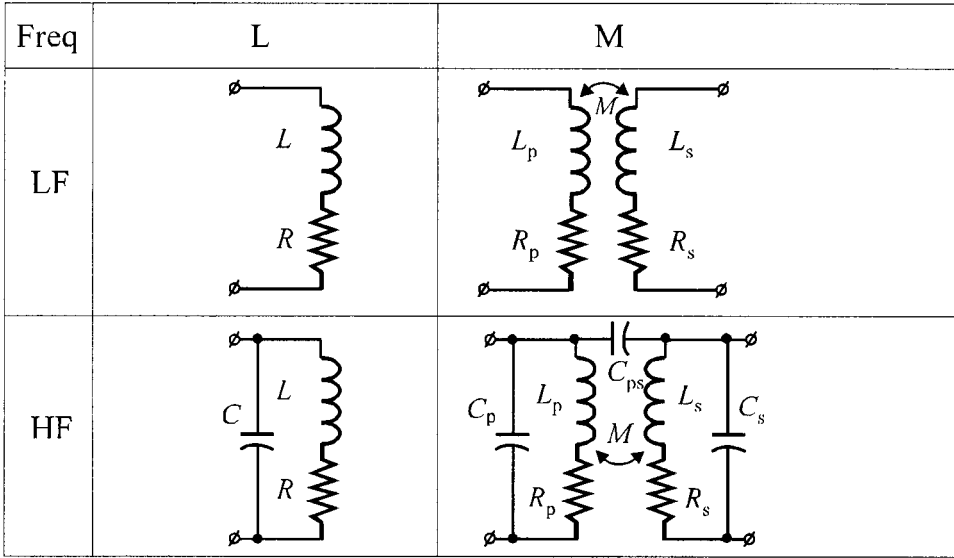


FIGURE 50.2 Basic equivalent circuits of inductive elements with self-inductance L , mutual inductance M for low (LF) and high (HF) frequencies.

$$v_s = N_s \frac{d\Phi}{dt} = \pm k \sqrt{L_p L_s} \frac{di_p}{dt} = \pm M \frac{di_p}{dt} \quad (50.2)$$

where $\pm k$ is the coupling coefficient of the primary (p) and secondary (s) windings. Its sign depends on the direction of the windings. Because of the similarity between Equations 50.1 and 50.2, mutual inductance is defined similarly to self-inductance. The definitions of self-inductance and mutual inductance described above are correct when L and M can be assumed constant, i.e., not depending on current, frequency, or time.

50.2 Equivalent Circuits and Inductive Element Models

Equivalent circuits of inductive elements and their mathematical models are built on the basis of analysis of energy processes in the elements. They are as follows: energy storage in the parts of the circuits represented by lumped inductances (L) and capacitances (C), and dissipation of energy in the parts of the circuits represented by lumped resistances (R). Essentially, the above-mentioned energy processes are never lumped, so the equivalent circuits and mathematical models of inductive elements only approximate reality. Choosing an equivalent circuit (model), one can influence the quality of the approximation. In Figure 50.2, the basic models of typical coreless inductive elements of electric circuits are presented, using the type of inductance (self-inductance L , mutual inductance M) and frequency band (low LF, high HF) as criteria. Models of inductive elements with ferromagnetic cores and problems concerning model parameter evaluation are beyond the scope of this chapter. The equivalent circuits of coreless inductive elements at low frequencies contain only inductances and series resistances. At high frequencies, parallel and coupling equivalent capacitances are included. Calculations of LCR values of complicated equivalent circuits (with many LCR elements) are very tedious, so often for that purpose a special dedicated processor with appropriate software is provided in the measuring device.

In metrology, complex notation [1] is frequently used to describe linear models of inductive elements. In complex notation, the impedances and transmittances are as follows:

$$Z = R_z + jX_z = Z_m \exp(j\phi_z), \quad Z_m = \sqrt{R_z^2 + X_z^2}, \quad \phi_z = \arctan \frac{X_z}{R_z} \quad (50.3)$$

$$T = R_T + jX_T = T_m \exp(j\phi_T), \quad T_m = \sqrt{R_T^2 + X_T^2}, \quad \phi_T = \arctan \frac{X_T}{R_T} \quad (50.4)$$

The components of impedances and transmittances can be described as algebraic functions of the *LCR* elements determined for the equivalent circuit. In each case, the forms of the functions depend on the assumed equivalent circuit. By measuring the real and imaginary components or modules and phase angles of impedances or transmittances and comparing them to corresponding quantities determined for the equivalent circuit, and then solving the obtained algebraic equations, the *LCR* values of the equivalent circuit can be determined.

An example for the *LF* equivalent circuit in Figure 50.2 can be obtained:

$$Z = R + j\omega L = R_z + jX_z \rightarrow R = R_z, \quad \omega L = X_z \quad (50.5)$$

$$T = j\omega M = R_T + jX_T \rightarrow R_T = 0, \quad \omega M = X_T \quad (50.6)$$

For the *HF* equivalent circuits shown in Figure 50.2, the models are more complex. More particularly, models of circuits with mutual inductance can represent:

- Ideal transformers, with only their self-inductances and mutual inductances of the coils
- Perfect transformers, without losses in the core
- Real transformers, having a specific inductance, resistance, and capacity of the coils, and also a certain level of losses in the core

The quality factor Q and dissipation factor D are defined for the equivalent circuits of inductive elements. In the case of a circuit with inductance and resistance only, they can be defined as follows:

$$Q = \frac{1}{D} = \frac{\omega L}{R} = \tau \omega \quad (50.7)$$

where parameter τ is a time constant.

The presented models with lumped inductance are not always a sufficiently good approximation of the real properties of electric circuits. This particularly applies to circuits made with geometrically large wires (i.e., of a significant length, surface area, or volume). In such cases, the models applied use an adequately distributed inductance (linearly, over the surface, or throughout the volume). Inductances determined to be the coefficients of such models depend on the geometrical dimensions and, in the case of surface conductivity or conduction by the surface or volume, by the frequencies of the currents flowing in the conductor lines.

A complex formulation is used to represent and analyze circuits with lumped and linear inductances. Sometimes the same thing can be done using simple linear differential equations or the corresponding integral operators.

The analytical methodology for such circuits is described in [1]. In the case of nonlinear inductances, the most frequently used method is the linearized equivalent circuit, also represented in a simplified form using a complex formulation. Circuits with distributed inductance are represented by partial differential equations.

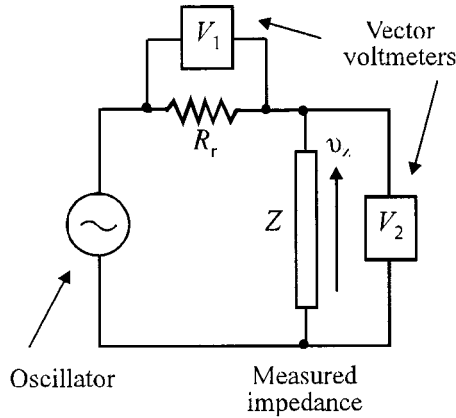


FIGURE 50.3 Circuit diagram for impedance measurement by current and voltage method.

50.3 Measurement Methods

Impedance (or transmittance) measurement methods for inductors are divided into three basic groups:

1. Current and voltage methods based on impedance/transmittance determination.
2. Bridge and differential methods based on comparison of the voltages and currents of the measured and reference impedances until a state of balance is reached.
3. Resonance methods based on physical connection of the measured inductor and a capacitor to create a resonant system.

Current–Voltage Methods

Current–voltage measurement methods are used for all types of inductors. A current–voltage method using vector voltmeters is shown in Figure 50.3. It is based on evaluation of the modules and phase angles of impedances (in the case of self-inductance) or transmittances (in the case of mutual inductance) using Equations 50.8 and 50.9

$$Z = \frac{v_2}{i} = R_r \frac{v_2}{v_1} = R_r \frac{V_{m2} \exp(j\phi_2)}{V_{m1} \exp(j\phi_1)} = R_r \frac{V_{m2}}{V_{m1}} \exp j(\phi_2 - \phi_1) = Z_m \exp(j\phi_z) \quad (50.8)$$

$$T = \frac{v_s}{i_p} = R_r \frac{v_s}{v_{pr}} = R_r \frac{V_{ms} \exp(j\phi_s)}{V_{mpr} \exp(j\phi_{pr})} = R_r \frac{V_{ms}}{V_{mpr}} \exp j(\phi_s - \phi_{pr}) = T_m \exp(j\phi_T) \quad (50.9)$$

where R_r = Sampling resistor used for measurement of current

v_1 = Voltage proportional to the current

v_2 = Voltage across the measured impedance

v_{pr} = Voltage proportional to primary current

v_s = Voltage of the secondary winding of the circuit with mutual inductance

A block diagram illustrating the principle of the vector voltmeter is shown in Figure 50.4a. The system consists of the multiplier or gated synchronous phase-sensitive detector (PSD) [3, 4] of the measured

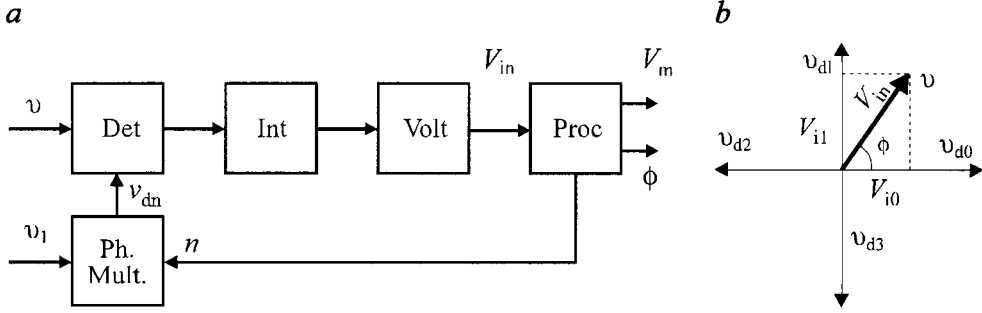


FIGURE 50.4 Block diagram (a) and phasor diagram (b) illustrating the principle of operation of a vector voltmeter. Block abbreviations: “Det” — phase-sensitive amplitude detector, “Int” — integrator, “Volt” — voltmeter, “Proc” — processor, “Ph. mult” — controlled phase multiplexer.

voltage v with the switching system of the phase of the reference voltage v_{dn} , integrator, digital voltmeter, and processor. The principle of vector voltmeter operation is based on determination of the magnitude V_m and phase angle ϕ of the measured voltage v in reference to voltage v_1 , which is proportional to the current i . Assume that voltages v and v_{dn} are in the following forms:

$$v = V_m \sin(\omega t + \phi) = V_m (\sin \omega t \cos \phi + \cos \omega t \sin \phi) \quad (50.10)$$

$$v_{dn} = V_{m_d} \sin\left(\omega t + n \frac{\pi}{2}\right), \quad n = 0, 1, 2, 3 \quad (50.11)$$

Phase angle $n\pi/2$ of voltage v_{dn} can take values from the set $\{0, \pi/2, \pi, 3/2 \pi\}$ by choosing the number n that gives the possibility of detecting the phase angle ϕ in all four quadrants of the Cartesian coordinate system, as is shown in Figure 50.4b. A multiplying synchronous phase detector multiplies voltages v and v_{dn} and bilinearly, and the integrator averages the multiplication result during time T_i .

$$V_{in} = \frac{1}{T_i} \int_0^{T_i} v v_{dn} dt \quad (50.12)$$

Averaging time $T_i = k T$, $k = 1, 2, 3 \dots$ is a multiple of the period T of the measured voltage. From Equations 50.10 through 50.12, an example for $0 \leq \phi \leq \pi/2$ (e.g., $n = 0$ and $n = 1$), a pair of numbers is obtained:

$$V_{i0} = 0.5 V_m V_{m_d} \cos \phi, \quad V_{i1} = 0.5 V_m V_{m_d} \sin \phi \quad (50.13)$$

which are the values of the Cartesian coordinates of the measured voltage v . The module and phase angle of voltage are calculated from:

$$V_m = \frac{2}{V_{m_d}} \sqrt{V_{i0}^2 + V_{i1}^2}, \quad \phi = \arctan \frac{V_{i1}}{V_{i0}} \quad (50.14)$$

Both coordinates of the measured voltage v can be calculated in a similar way in the remaining quadrants of the Cartesian coordinate system. A vector voltmeter determines the measured voltage as vector (phasor) by measurement of its magnitude and angle as shown in Figure 50.4.

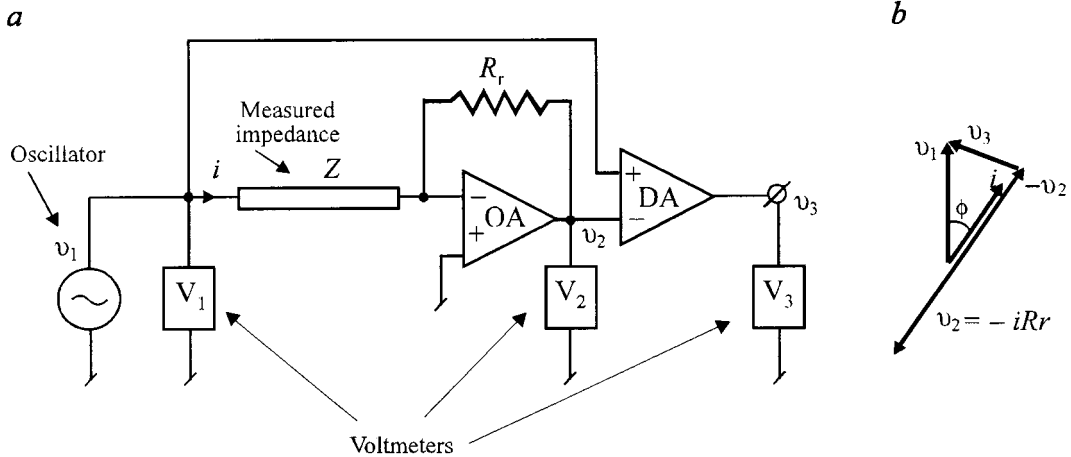


FIGURE 50.5 Block diagram (a) and phasor diagram (b) of the “three-voltmeter” method. Operational and differential amplifiers are represented by blocks “OA” and “DA.”

The current and voltage method of impedance or transmittance measurement is based on measurement of voltages $v_1 = i R_r$ and v_2 or $v_{pr} = i R_r$ and v_s , and the use of Equations 50.8 or 50.9. Calculation of the voltage measurement results and control of number n is performed by a processor. References [11–13] contain examples of PSD and vector voltmeter applications. Errors of module and phase angle measurement of impedance when using vector voltmeters are described in [11] as being within the range of 1% to 10% and between 10^{-5} rad and 10^{-3} rad, respectively, for a frequency equal to 1.8 GHz. Publications [9] and [10] contain descriptions of applications of comparative methods which have had an important influence on the development of the methods.

Another method of comparative current/voltage type is a modernized version of the “three-voltmeter” method [7]. A diagram of a measurement system illustrating the principle of the method is shown in Figure 50.5a and b.

The method is based on the properties of an operational amplifier (OA), in which output voltage v_2 is proportional to input voltage v_1 and to the ratio of the reference resistance R_r to measured impedance Z . The phasor difference v_3 of voltages v_1 and v_2 can be obtained using the differential amplifier (DA). The three voltages (as in Figure 50.5b) can be used for the module Z_m and phase ϕ calculation using relations:

$$v_2 = -i R_r = -\frac{R_r}{Z} v_1 \rightarrow Z_m = \frac{V_1}{V_2} R_r \quad (50.15)$$

$$v_3 = v_1 - v_2 \rightarrow \phi = \arccos \frac{V_1^2 + V_2^2 - V_3^2}{2V_1 V_2} \quad (50.16)$$

where V_1, V_2, V_3 are the results of rms voltage measurements in the circuit. The advantage of the method lies in limiting the influence of stray capacitances as a result of attaching one of the terminals of the measured impedance to a point of “virtual ground.” However, to obtain small measurement errors, especially at high frequencies, amplifiers with very good dynamic properties must be used.

Joint errors of inductance measurement, obtained by current and voltage methods, depend on the following factors: voltmeter errors, errors in calculating resistance R_r , system factors (residual and leakage inductances, resistances and capacitances), and the quality of approximation of the measured impedances by the equivalent circuit.

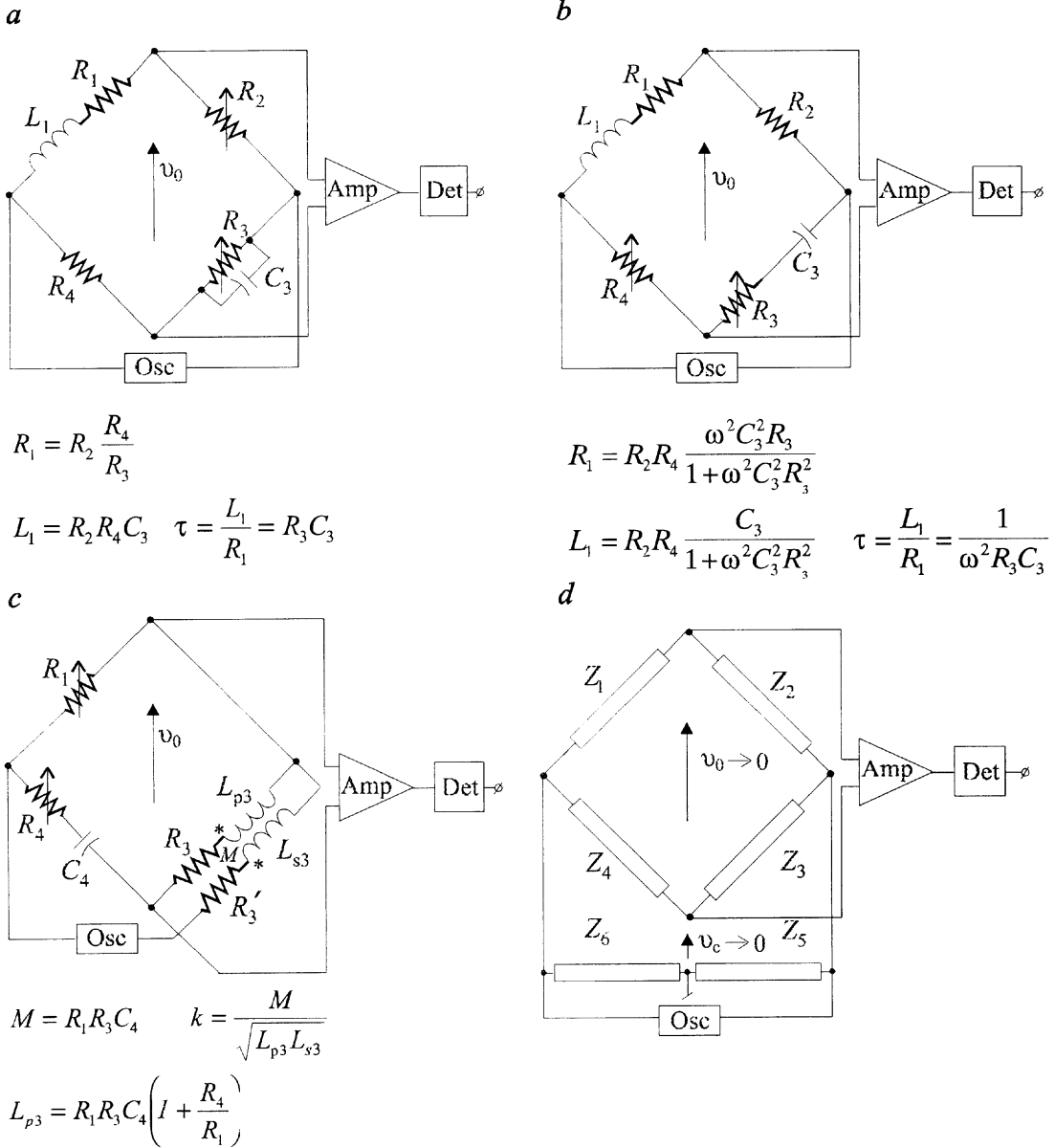


FIGURE 50.6 Bridge circuits used for inductance measurements: Maxwell-Wien bridge (a), Hay bridge (b), Carey-Foster bridge (c), and ac bridge with Wagner branch (d). Block abbreviations: “Osc” — oscillator, “Amp” — amplifier, “Det” — amplitude detector.

Bridge Methods

There are a variety of bridge methods for measuring inductances. Bridge principles of operation and their circuit diagrams are described in [2–5] and [7]. The most common ac bridges for inductance measurements and the formulae for calculating measurement results are shown in [Figure 50.6](#).

The procedure referred to as *bridge balancing* is based on a proper selection of the reference values of the bridge so as to reduce the differential voltage to zero (as referred to the output signal of the balance indicator). It can be done manually or automatically.

The condition of the balanced bridge $v_0 = 0$ leads to the following relation between the impedances of the bridge branches; one of them (e.g., Z_1) is the measured impedance:

$$Z_1 Z_3 = Z_2 Z_4 \rightarrow (R_1 + jX_1)(R_3 + jX_3) = (R_2 + jX_2)(R_4 + jX_4) \quad (50.17)$$

Putting Equation 50.17 into complex form and using expressions for the impedances of each branch, two algebraic equations are obtained by comparing the real and imaginary components. They are used to determine the values of the equivalent circuit elements of the measured impedance. In the most simple case, they are L and R elements connected in series. More complicated equivalent circuits need more equations to determine the equivalent circuit parameters. Additional equations can be obtained from measurements made at different frequencies.

In self-balancing bridges, vector voltmeters preceded by an amplifier of the out-of-balance voltage v_0 are used as “zero” detectors. The detector output is coupled with variable standard bridge components.

The Maxwell-Wien bridge shown in Figure 50.6a is one of the most popular ac bridges. Its range of measurement values is large and the relative error of measurement is about 0.1% of the measured value. It is used in the wide-frequency band 20 Hz to 1 MHz. The bridge is balanced by varying the R_2 and R_3 resistors or by varying R_3 and capacitor C_3 . Some difficulties can be expected when balancing a bridge with inductors with high time constants.

The Hay bridge presented in Figure 50.6b is also used for measurement of inductors, particularly those with high time constants. The balance conditions of the bridge depend on the frequency value, so the frequency should be kept constant during the measurements, and the bridge supply voltage should be free from higher harmonic distortions. The dependence of bridge balance conditions on frequency also limits the measurement ranges. The bridge is balanced by varying R_3 and R_4 resistors and by switching capacitor C_3 .

Mutual inductance M of two windings with self-inductances L_p and L_s can be determined by Maxwell-Wien or Hay bridges. For this, two inductance measurements have to be made for two possible combinations of the series connection of both coupled windings: one of them for the corresponding directions of the windings, and one for the opposite directions. Two values of inductances L_1 and L_2 are obtained as the result of the measurements:

$$L_1 = L_p + L_s + 2 M, \quad L_2 = L_p + L_s - 2 M \quad (50.18)$$

Mutual inductance is calculated from:

$$M = 0.25(L_1 - L_2) \quad (50.19)$$

The Carey-Foster bridge described in Figure 50.6c is used for mutual inductance measurement. The self-inductances of the primary and secondary windings can be determined by two consecutive measurements. The expressions presented in Figure 50.6c yield the magnetic coupling coefficient k . The bridge can be used in a wide frequency range. The bridge can be balanced by varying R_1 and R_4 resistances and switching the remaining elements.

For correct measurements when using ac bridges, it is essential to minimize the influence of harmful couplings among the bridge elements and connection wires, between each other and the environment. Elimination of parallel (common) and series (normal) voltage distortions is necessary for high measurement resolution. These couplings are produced by the capacitances, inductances, and parasitic resistances of bridge elements to the environment and among themselves. Because of their appearance, they are called stray couplings. Series voltage distortions are induced in the bridge circuit by varying common electromagnetic fields. Parallel voltage distortions are caused by potential differences between the reference point of the supply voltage and the points of the out-of-balance voltage detector system.

Magnetic shields applied to connection wires and bridge-balancing elements are the basic means of minimizing the influence of parasitic couplings and voltage distortions [8]. All the shields should be connected as a “star” connection; that is, at one point, and connected to one reference (“ground”) point of the system. For these reasons, amplifiers of out-of-balance voltage with symmetric inputs are frequently used in ac bridges, as they reject parallel voltage distortions well.

When each of the four nodes of the bridge has different stray impedances to the reference ground, an additional circuit called a Wagner branch is used (see Figure 50.6*d*). By varying impedances Z_5 and Z_6 in the Wagner branch, voltage v_c can be reduced to zero; by varying the other impedances, voltage v_0 can also be reduced to zero. In this way, the bridge becomes symmetrical in relation to the reference ground point and the influence of the stray impedances is minimized.

The joint error of the inductance measurement results (when using bridge methods) depends on the following factors: the accuracy of the standards used as the bridge elements, mainly standard resistors and capacitors; errors of determining the frequency of the bridge supplying voltage (if it appears in the expressions for the measured values); errors of the resolution of the zero detection systems (errors of state of balance); errors caused by the influence of residual and stray inductances; resistances and capacitances of the bridge elements and wiring; and the quality of approximation of the measured impedances in the equivalent circuit.

The errors of equivalent resistance measurements of inductive elements using bridge methods are higher than the errors of inductance measurements. The number of various existing ac bridge systems is very high. Often the bridge system is built as a universal system that can be configured for different applications by switching elements. One of the designs of such a system is described in [3]. Reference [13] describes the design of an automatic bridge that contains, as a balancing element, a multiplying digital-to-analog converter (DAC), controlled by a microcontroller.

Differential Methods

Differential methods [7] can be used to build fully automatic digital impedance meters (of real and imaginary components or module and phase components) that can also measure inductive impedances. Differential methods of measurement are characterized by small errors, high resolution, and a wide frequency band, and often utilize precise digital control and digital processing of the measurement results. The principle of differential methods is presented through the example of a measuring system with an inductive voltage divider and a magnetic current comparator (Figure 50.7). An inductive voltage divider (IVD) is a precise voltage transformer with several secondary winding taps that can be used to vary the secondary voltage in precisely known steps [7]. By combining several IVDs in parallel, it is possible to obtain a precise voltage division, usually in the decade system. The primary winding is supplied from a sinusoidal voltage source. A magnetic current comparator (MCC) is a precise differential transformer with two primary windings and a single secondary winding. The primary windings are connected in a differential way; that is, the magnetic fluxes produced by the currents in these windings subtract. The output voltage of the secondary winding depends on the current difference in the primary windings. MCCs are characterized by very high resolution and low error but are expensive. In systems in common use, precise control of voltages (IVD) is provided by digitally controlled (sign and values) digital voltage dividers (DVD), and the magnetic comparator is replaced by a differential amplifier.

The algorithms that enable calculation of L and R element values of the series equivalent circuit of an inductive impedance Z in a digital processor result from the mathematical model described in Figure 50.7. When the system is in a state of equilibrium, the following relations occur:

$$v_0 = 0 \rightarrow i_z - i_r = 0 \quad (50.20)$$

$$i_z = v_1 \frac{1}{R + j\omega L}, \quad i_r = D_r v_1 \left(\frac{b}{R_r} - aj\omega C_r \right) \quad (50.21)$$

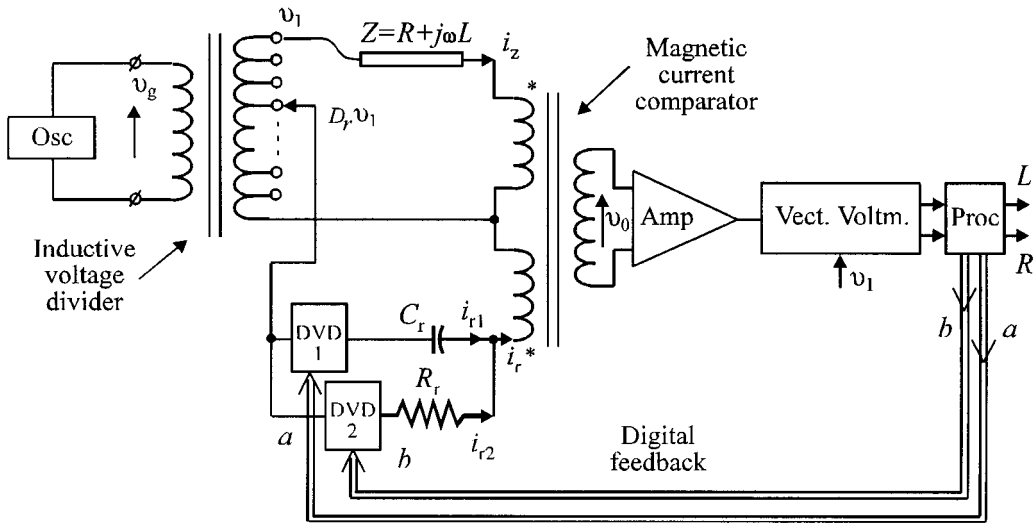


FIGURE 50.7 Scheme of the differential method. Block abbreviations: “Osc”, “Amp” — as in Figure 50.6, “Vect. voltm” — vector voltmeter, “Proc” — processor, “DVD” — digital voltage divider.

where $0 < D_r \leq 1$ is the coefficient of v_1 voltage division and the values a and b are equivalent to the binary signals used by the processor to control DVD. Multiple digital-to-analog converters (DACs) are used as digitally controlled voltage dividers. They multiply voltage $D_r v_1$ by negative numbers ($-a$), which is needed in the case of using a standard capacitor C_r for measurements of inductance. After substituting Equation 50.21 into Equation 50.20 and equating the real and imaginary parts, the following formulae are obtained:

$$L = \frac{a R_r^2 C_r}{D_r (b^2 + a^2 \omega^2 R_r^2 C_r^2)} \quad (50.22)$$

$$R = \frac{b R_r}{D_r (b^2 + a^2 \omega^2 R_r^2 C_r^2)} \quad (50.23)$$

The lengths N of the code words $\{a_n\} \leftrightarrow a$ and $\{b_n\} \leftrightarrow b$, $n = 1, 2, \dots, N$ determine the range and resolution of the measurement system; that is, the highest measurable inductance and resistance values and the lowest detectable values. The range can be chosen automatically by changing the division coefficients D_r . Achieved accuracy is better than 0.1% in a very large range of impedances and in a sufficiently large frequency range. Measurements can be periodically repeated and their results can be stored and processed.

Resonance Methods

Resonance methods are a third type of inductance measurement method. They are based on application of a series or parallel resonance LC circuits as elements of either a bridge circuit or a two-port (four-terminal) “T”-type network. Examples of both circuit applications are presented in Figure 50.8.

In the bridge circuit shown in Figure 50.8a, which contains a series resonance circuit, the resonance state is obtained by varying the capacitor C_r , and then the bridge is balanced ($v_0 = 0$) using the bridge resistors. From the resonance and balance conditions, the following expressions are obtained:

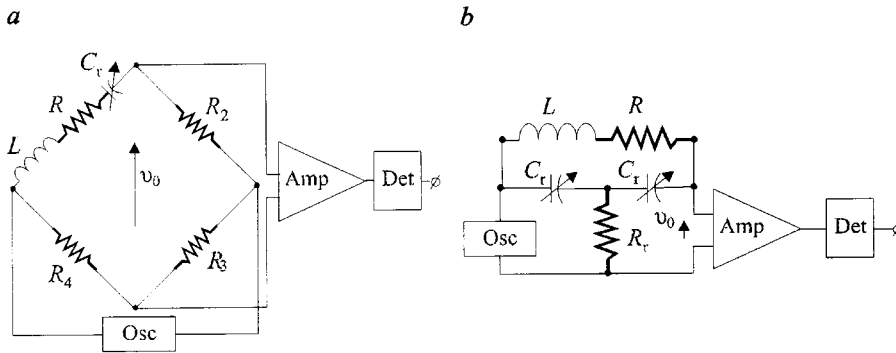


FIGURE 50.8 Circuits diagrams applied in resonance methods: bridge circuit with series resonance circuit (a), and two-port “shunted T” type with parallel resonance circuit (b). Block abbreviations as in Figure 50.6.

$$L = \frac{1}{\omega^2 C_r}, \quad R = R_2 \frac{R_4}{R_3} \quad (50.24)$$

To calculate the values of the LR elements of the series equivalent circuit of the measured impedance, it is necessary to measure (or know) the angular frequency ω of the supply voltage. The frequency band is limited by the influence of unknown interturn capacitance value. In the “shunted T” network presented in Figure 50.8b, the state of balance (i.e., the minimal voltage v_0 value) is achieved by tuning the multiloop LCR circuit to parallel resonance. The circuit analysis [7] is based on the “star-delta” transformation of the $C_r R_r C_r$ element loop and leads to the relations for L and R values:

$$L = \frac{2}{\omega^2 C_r}, \quad R = \frac{1}{\omega^2 C_r^2 R_r} \quad (50.25)$$

According to reference [7], a “double T” network can be used for inductive impedance measurements at high frequencies (up to 100 MHz).

50.4 Instrumentation

Instruments commonly used for inductance measurements are built as universal and multifunctional devices. They enable automatic (triggered or cyclic) measurements of other parameters of the inductive elements: capacitance, resistance, quality, and dissipation factors. Equipped with interfaces, they can also work in digital measuring systems. Table 50.1 contains a review of the basic features of the instruments called LCR meters, specified on the basis of data accessible from the Internet [15]. Proper design of LCR meters limits the influence of the factors causing errors of measurement (i.e., stray couplings and distortions). The results of inductance measurements also depend on how the measurements are performed, including how the measured inductor is connected to the meter. Care should be taken to limit such influences as inductive and capacitive couplings of the inductive element to the environment, sources of distortion, and the choice of operating frequency.

TABLE 50.1 Basic Features of Selected Types of LCR Meters

Manufacturer, model (designation)	Measurement range of inductance	Frequency	Basic accuracy	Price
Leader LCR 740 (LCR bridge)	0.1 μ H–1100 H	int. 1 kHz ext. 50 Hz–40 kHz	0.5%	\$545
Electro Scientific Industries 253 (Digital impedance meter)	200 μ H–200 H	1 kHz	(3.5 digit)	\$995
Stanford RS SR 715 (LCR meter)	0.1 nH–100 kH	100 Hz–10 kHz	0.2%	\$1295 (\$1425)
Wayne Kerr 4250	0.01 nH–10 kH	120 Hz–100 kHz	0.1%	\$3500
General Radio 1689 (Precision LCR meter)	0.00001 mH–99.999 H	12 Hz–100 kHz	0.02%	\$4120
Hewlett-Packard 4284A (Precision LCR meter)	0.01 nH–99.9999 kH	20 Hz–1 MHz	0.05%	\$9500

References

1. R. C. Dorf, *Introduction to Electric Circuits*, New York: John Wiley & Sons, 1989.
2. J. P. Bentley, *Principles of Measurement Systems, 2nd ed.*, Harlow: Longman Group U.K., New York: John Wiley & Sons, 1988.
3. A. D. Helfrick and W. D. Cooper, *Modern Electronic Instrumentation and Measurement Techniques*, Englewood Cliffs, NJ: Prentice-Hall, 1990.
4. L. D. Jones and A. F. Chin, *Electronic Instruments and Measurements, 2nd ed.*, Englewood Cliffs, NJ: Prentice-Hall, 1991.
5. M. U. Reissland, *Electrical Measurement*, New York: John Wiley & Sons, 1989.
6. P. H. Sydenham (ed.), *Handbook of Measurement Science, Vol. 1, Theoretical Fundamentals*, New York: John Wiley & Sons, 1982.
7. P. H. Sydenham (ed.), *Handbook of Measurement Science, Vol. 2, Practical Fundamentals*, New York: John Wiley & Sons, 1983.
8. R. L. Bonebreak, *Practical Techniques of Electronic Circuit Design, 2nd ed.*, New York: John Wiley & Sons, 1987.
9. S. Hashimoto and T. Tamamura, An automatic wide-range digital LCR meter, *Hewlett-Packard J.*, 8, 9–15, 1976.
10. T. Wakasugi, T. Kyo, and T. Tamamura, New multi-frequency LCZ meters offer higher-speed impedance measurements, *Hewlett-Packard J.*, 7, 32–38, 1983.
11. T. Yonekura, High-frequency impedance analyzer, *Hewlett-Packard J.*, 5, 67–74, 1994.
12. M. A. Atmanand, V. J. Kumar, and V. G. K. Murti, A novel method of measurement of L and C , *IEEE Trans. Instrum. Meas.*, 4, 898–903, 1995.
13. M. A. Atmanand, V. J. Kumar, and V. G. K. Murti, A microcontroller- based quasi-balanced bridge for the measurement of L , C and R , *IEEE Trans. Instrum. Meas.*, 3, 757–761, 1996.
14. J. Gajda and M. Szyper, Electromagnetic transient states in the micro resistance measurements, *Systems Analysis Modeling Simulation*, Amsterdam: Overseas Publishers Association, 22, 47–52, 1996.
15. Information from *Internet* on LCR meters.